Taylor & Francis
Taylor & Francis Group

BASIC RESEARCH PAPER

🔓 OPEN ACCESS

Essential control of mitochondrial morphology and function by chaperone-mediated autophagy through degradation of PARK7

Bao Wang[†], Zhibiao Cai[†], Kai Tao, Weijun Zeng, Fangfang Lu, Ruixin Yang, Dayun Feng, Guodong Gao, and Qian Yang

Department of Neurosurgery, Tangdu Hospital, The Fourth Military Medical University, Xi'an, Shaanxi, China

ABSTRACT

As a selective degradation system, chaperone-mediated autophagy (CMA) is essential for maintaining cellular homeostasis and survival under stress conditions. Increasing evidence points to an important role for the dysfunction of CMA in the pathogenesis of Parkinson disease (PD). However, the mechanisms by which CMA regulates neuronal survival under stress and its role in neurodegenerative diseases are not fully understood. *PARK7/DJ-1* is an autosomal recessive familial PD gene. PARK7 plays a critical role in antioxidative response and its dysfunction leads to mitochondrial defects. In the current study, we showed that CMA mediated the lysosome-dependent degradation of PARK7. Importantly, CMA preferentially removed the oxidatively damaged nonfunctional PARK7 protein. Furthermore, CMA protected cells from mitochondrial toxin MPP$^+$-induced changes in mitochondrial morphology and function, and increased cell viability. These protective effects were lost under PARK7-deficiency conditions. Conversely, overexpression of PARK7 significantly attenuated the mitochondrial dysfunction and cell death exacerbated by blocking CMA under oxidative stress. Thus, our findings reveal a mechanism by which CMA protects mitochondrial function by degrading nonfunctional PARK7 and maintaining its homeostasis, and dysregulation of this pathway may contribute to the neuronal stress and death in PD pathogenesis.

Introduction

Parkinson disease (PD) is characterized by the progressive death of dopaminergic (DA) neurons in the substantia nigra pars compacta.[1] Mitochondrial dysfunction and oxidative stress have been recognized to play a significant role in the nigral neuronal death in PD.[2] Increasing evidence points to the dysregulation of protein homeostasis as a critical component in triggering the neurodegenerative process.[3,4] However, the critical mechanisms responsible for protein dys-homeostasis and neuronal death resulting from it are complex and remain to be fully understood.

Emerging evidence indicates that dysregulation of autophagy may contribute to the pathogenic process in PD.[5,6] Multiple genetic risk factors associated with PD have been linked to 2 common forms of autophagy, macroautophagy and chaperone-mediated autophagy (CMA).[7] CMA process involves the binding of HSPA8/HSC70 (heat shock protein 8), to selected protein substrates and their delivery to the lysosomal membrane, where they interact with membrane receptor LAMP2A (lysosomal-associated membrane protein 2A).[8,9] Several studies have established a strong connection between CMA and PD. PD genetic risk factors SNCA (synuclein, α) and LRRK2 (leucine-rich repeat kinase 2) are CMA substrates.[10,11] The PD causing mutants of these proteins seem to block the CMA process. A

mutant of *UCHL1* (ubiquitin carboxyl-terminal hydrolase L1), another gene whose mutation causes familial PD, also reduces CMA activity.[12,13] In addition, CMA maintains the homeostasis of MEF2D (myocyte enhancer factor 2D), a factor critical for the survival of dopaminergic neurons.[14-16] Analysis of postmortem brain specimens from PD patients shows that the level of LAMP2A in the substantia nigra pars compacta is reduced compared to the controls.[17] Together, these findings suggest that inhibition CMA activity is a cellular effect shared by multiple factors associated with PD and dysfunction of this process may underlie the pathogenesis of the disease.

PARK7 (Parkinson disease [autosomal recessive, early onset] 7) is a multifunctional protein involved in various cellular activities. One of its principle functions is antioxidative defense and maintains mitochondrial homeostasis.[18,19] Increasing PARK7 level protects mitochondrial function and promotes cell survival.[20,21] PARK7 functions as a homodimer. Mutations in PARK7, which is associated with autosomal recessive early-onset Parkinson disease, destroy its dimeric structure and activity, and impair mitochondrial function.[22,23] Analysis of postmortem brains of PD patients reveals a significant accumulation of the extensively oxidized and damaged PARK7.[24] However, the mechanisms responsible for such an accumulation remain unknown. Nor is it clear whether dysfunction of

---

CONTACT Qian Yang ✉ qianyang@fmmu.edu.cn; Guodong Gao ✉ gguodong@fmmu.edu.cn 🖅 Department of Neurosurgery, Tangdu Hospital, The Fourth Military Medical University, 569 Xinsi Road, Xi'an, Shaanxi 710038, China.

Color versions of one or more of the figures in the article can be found online at www.tandfonline.com/kaup.

[†]These authors contributed equally to this study.

🔂 Supplemental data for this article can be accessed on the publisher's website.

a protein degradation pathway may directly affect PARK7 and mitochondrial function.

Here we show that CMA plays an important and direct role in modulating PARK7 by controlling its turnover. Importantly, CMA appears to preferentially target the oxidatively damaged and nonfunctional PARK7 to the lysosomes for removal. Regulation of PARK7 by CMA plays a role in maintaining mitochondrial function and morphology. Reducing CMA activity leads to the accumulation of inactive PARK7 and disrupts mitochondrial function. Thus, CMA regulates mitochondrial function via maintaining PARK7 homeostasis.

Results

Degradation of PARK7 by lysosomes

As an antioxidative protein, PARK7 plays a central role in limiting mitochondrial damage in response to oxidative stress. PARK7 deficiency leads to multiple mitochondrial abnormalities.[25,26] Because the PARK7 amino acid sequence contains multiple putative CMA recognition motifs including a perfect canonical one (I91 to Q95) (Fig. S1), we investigated the possibility of whether PARK7 stability may be regulated by lysosomes via CMA pathway. To test the role of lysosomes in PARK7 degradation, we inhibited lysosomal hydrolase activities by exposing SN4741 cells, a mouse midbrain dopamine neuron progenitor cell line,[27] to a combination of NH_4Cl and leupeptin (Leup). This led to a dose-dependent increase in PARK7 levels (Fig. 1A), indicating that PARK7 levels may be regulated by lysosomes. To assess whether autophagy is involved in regulation of PARK7, we treated cells with long-term serum deprivation, which activates CMA (Fig. S2),[28] and found that this caused a reduction in PARK7 levels. Application of a combination of NH_4Cl and leupeptin (Leup) reversed the decrease in PARK7 levels induced by long-time serum withdrawal (Fig. 1B). Immunofluorescence for LAMP1, a known marker for lysosomes, and PARK7 revealed that PARK7 association with lysosomal compartment was increased following combinatorial treatment of serum deprivation and NH_4Cl with leupeptin (Leup) (Fig. 1C). In contrast, treating cells with the macroautophagy inhibitor 3-methyladenine (3-MA), which effectively suppressed macroautophagy activity, as indicated by the reduced level of MAP1LC3B-II and the augmented level of the macroautophagy substrate SQSTM1, failed to significantly alter the PARK7 level (Fig. 1D). Similarly, 3-MA also failed to reverse serum withdrawal-induced decrease of PARK7 (Fig. 1E). MG-132, a proteasome inhibitor that caused significant accumulation of ubiquitinated proteins, had little effect on the levels of PARK7 (Fig. 1F). Together, these data indicate that lysosomes but not the ubiquitin proteasome is the primary mechanism that controls PARK7 degradation. Furthermore, this degradation may involve a non-macroautophagy mechanism.

Regulation of PARK7 by CMA

Chaperone protein HSPA8 directly binds CMA substrate proteins and targets them to the lysosomes for LAMP2A-mediatd degradation.[29] To establish PARK7 as a CMA substrate, we immunoprecipitated the endogenous HSPA8 from the cytosolic lysates of SN4741 cells or from HEK293 cellular lysates overexpressing PARK7, and blotted for the bound PARK7 (the full blot is shown in Fig. S3). This analysis showed that both endogenous PARK7 and Flag-PARK7 coimmunoprecipitated with HSPA8 (Fig. 2A). Consistent with this, overexpression of LAMP2A, whose modulation correlated closely with CMA (Fig. S4), the rate-limiting factor for the entire CMA process,[30,31] significantly decreased the PARK7 levels. Cotreatment with NH_4Cl and leupeptin (Leup) prevented PARK7 from LAMP2A-induced degradation (Fig. 2B and C). Conversely, reducing LAMP2A protein by shRNA-Lamp2a increased the level of PARK7 (Fig. 2D). Overexpression of LAMP2A had no effect on the mRNA level of Park7 (Fig. S5). We then tested PARK7 by lysosomal binding and uptake assays, a gold standard for confirming a protein as CMA substrate. We purified lysosomes from rat liver following starvation and showed that the lysosomal faction was largely devoid of ER and mitochondrial markers, intact, and enriched for makers of active CMA (Figs. S6 and S7). We incubated the HEK293 lysates containing overexpressed Flag-PARK7 or purified PARK7 with the lysosomal preparation, and after washing, immunoblotted for the presence of PARK7. This analysis showed that a significant amount of PARK7 was associated with or present inside the lysosomes (Fig. 2E). Coincubation of PARK7 lysates with the increased amount of purified RNase A, a known CMA substrate protein, dose-dependently reduced the amounts of PARK7 associated with or taken up by the lysosomes (Fig. 2F). We mutated the amino acid residues Q95E or N144R within the putative CMA motifs in PARK7 ($I^{91}LKEQ^{95}$ and $N^{144}RVEK^{148}$) to Ala, and tested the effects of mutating either Q95E or N144R on the binding between PARK7 and HSPA8 by coimmunoprecipitation as described in Figure 2A. This analysis revealed that while mutating N144R did not significantly affect its binding to HSPA8, mutating Q95E clearly reduced the interaction between PARK7 and HSPA8 (Fig. 2G), indicating that $I^{91}LKEQ^{95}$ but not $N^{144}RVEK^{148}$ may be the primary CMA motif for PARK7. To corroborate with this finding, we overexpressed wild-type (WT) PARK7, QE→AA or NR→AA, and subjected cells to serum withdrawal to activate CMA. This led to a significant decrease of WT and NR→AA Flag-PARK7. Inhibition of lysosomal protease activity by NH_4Cl and leupeptin (Leup) attenuated this decrease (Fig. 2H). In contrast, QE→AA Flag-PARK7 was much more resistant to serum withdrawal-induced degradation, indicating that changing QE to AA interferes with CMA-mediated degradation of the protein. Consistently, in lysosomal uptake assay, when compared to that of WT PARK7, the ratio of P.I. (+):P.I. (−) [P.I. (+):P.I. (−) is the ratio of uptake/binding and correlates positively with the rate of lysosomal degradation] in the QE→AA mutant is significantly reduced, indicating that QE→AA mutation is degraded by CMA at a much more reduced rate due to significantly decreased uptake by the lysosomes (Fig. 2I). Together, these results support the idea strongly that PARK7 is a direct CMA substrate and regulated effectively by this mode of autophagy.

Preferential degradation of oxidatively damaged PARK7 by CMA

Our previous studies have shown that CMA is activated to remove nonfunctional proteins and maintain cellular homeostasis under
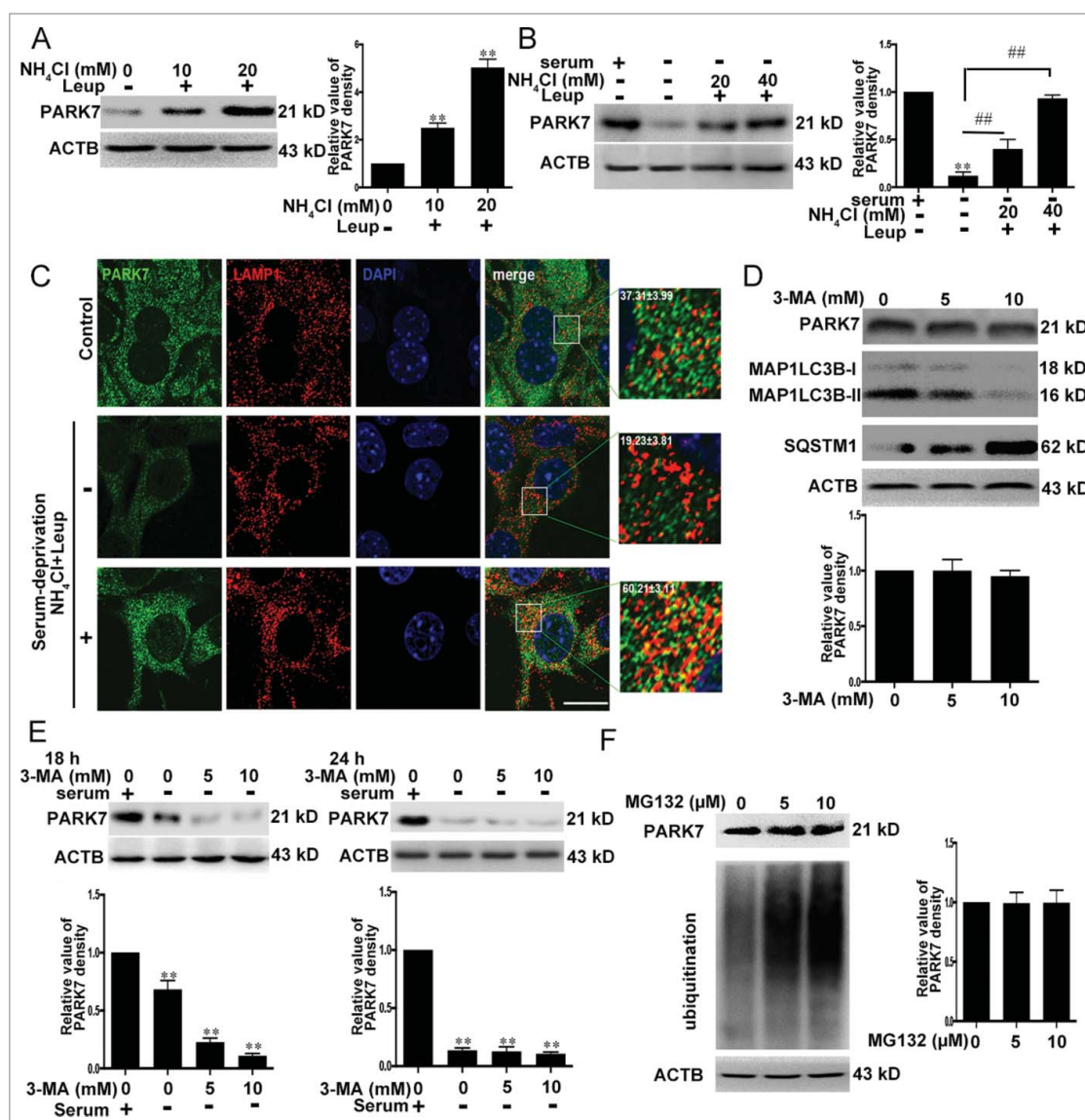
Figure 1. Degradation of PARK7 by lysosomes. (A) The effect of inhibition of lysosomal activity on PARK7. SN4741 cells were incubated with NH_4Cl and leupeptin (Leup; 100 μM used in this and subsequent experiments) for 18 h and the levels of PARK7 were analyzed by immunoblotting. The right graph shows the quantification of PARK7 levels (mean ± SEM, n = 3; **, $P < 0.01$ compared to the control group). (B) The effect of serum deprivation on PARK7. SN4741 cells were maintained in serum free medium in the absence or presence of NH_4Cl and Leupeptin (Leup) for 24 h. The levels of PARK7 were analyzed by immunoblotting. The right graph shows the quantification of PARK7 levels (mean ± SEM, n = 3; **, $P < 0.01$ compared to the control group; ##, $P < 0.01$ compared to serum-free only group). (C) The effect of serum deprivation on PARK7 and LAMP1 colocalization. SN4741 cells were treated as described in (B). The colocalization of PARK7 and LAMP1 was determined by immunofluorescence. The magnified images were provided. The ratio of colocalization was calculated. Scale bar: 50 μm. (D) The effect of 3-MA on PARK7. SN4741 cells were treated with 3-MA for 8 h and the levels of PARK7, MAP1LC3B-I/II and SQSTM1 were tested by immunoblotting. The lower graph shows the quantification of PARK7 level (mean ± SEM, n = 3). (E) The effect of 3-MA on serum withdrawal-induced decrease of PARK7. SN4741 cells were maintained in serum-free media with or without 3-MA for the indicated time and the levels of PARK7 were detected by immunoblotting. The lower graphs show the quantification of PARK7 levels (mean ± SEM, n = 3; **, $P < 0.01$ compared to the control group). (F) The effect of MG-132 on the level of PARK7. SN4741 cells were treated with the proteasome inhibitor MG132 for 8 h and the levels of PARK7 were determined by anti-ubiquitin (Ub) and anti-PARK7 blotting. The right graph shows the quantification of PARK7 levels (mean ± SEM, n = 3).

moderate oxidative stress such as a moderate dose of 1-methyl-4-phenylpyridinium (MPP$^+$).[15] We examined whether CMA degrades PARK7 under MPP$^+$-induced neurotoxic stress. These results showed that exposure to MPP$^+$ clearly reduced the level of PARK7 in SN4741 cells. Blocking CMA activity by shRNA-*Lamp2a* or lysosomal activity by NH_4Cl and leupeptin (Leup) significantly attenuated the MPP$^+$-induced decrease of the PARK7 level (Fig. 3B), these results suggest that MPP$^+$ reduces PARK7 primarily via CMA.

Previous studies have shown that CMA protects cells against oxidative stress by degrading oxidized proteins and oxidative stress can cause extensive oxidative modifications of PARK7 and inhibit PARK7 activity.[32] We tested how oxidative modification of PARK7 may affect its degradation by CMA. We treated SN4741 cells with MPP$^+$, immunoprecipitated endogenous PARK7, and then blotted the precipitated PARK7 for carbonyl oxidation using the OxyBlot protocol (see Materials and Methods). This analysis showed that MPP$^+$ treatment caused a significant increase in the level of carbonyl oxidation of PARK7. Reducing CMA activity by sh-*Lamp2a* under this condition significantly exacerbated the accumulation of oxidized PARK7 (Fig. 3C). Since mutant QE→AA is resistant to

CMA-mediated degradation (Fig. 2H), we compared the levels of oxidative modification of the QE→AA mutant. This analysis showed that oxidized QE→AA Flag-PARK7 accumulated at a higher rate than that of WT Flag-PARK7 following a brief MPP+ treatment (Fig. 3D). It is known that the PARK7 accumulated in the brains of PD patients shows a more acidic pI.[24] Also, oxidative stress causes PARK7 acidification.[33] We investigated how acidification of PARK7 affected its degradation by

CMA. Immunoblotting analysis following 2-dimensional SDS-PAGE revealed that MPP+ caused a significant increase in the level of the more acidic forms of PARK7 (pI 6.3) and inhibition of CMA by sh*Lamp2a* exacerbated this increase (Fig. 3E). Since PARK7 functions as a homodimer and extensive oxidative modifications disrupt its dimerization,[34] we tested how CMA activity affected the levels of the PARK7 monomer and dimer by treating soluble lysates with the covalent chemical
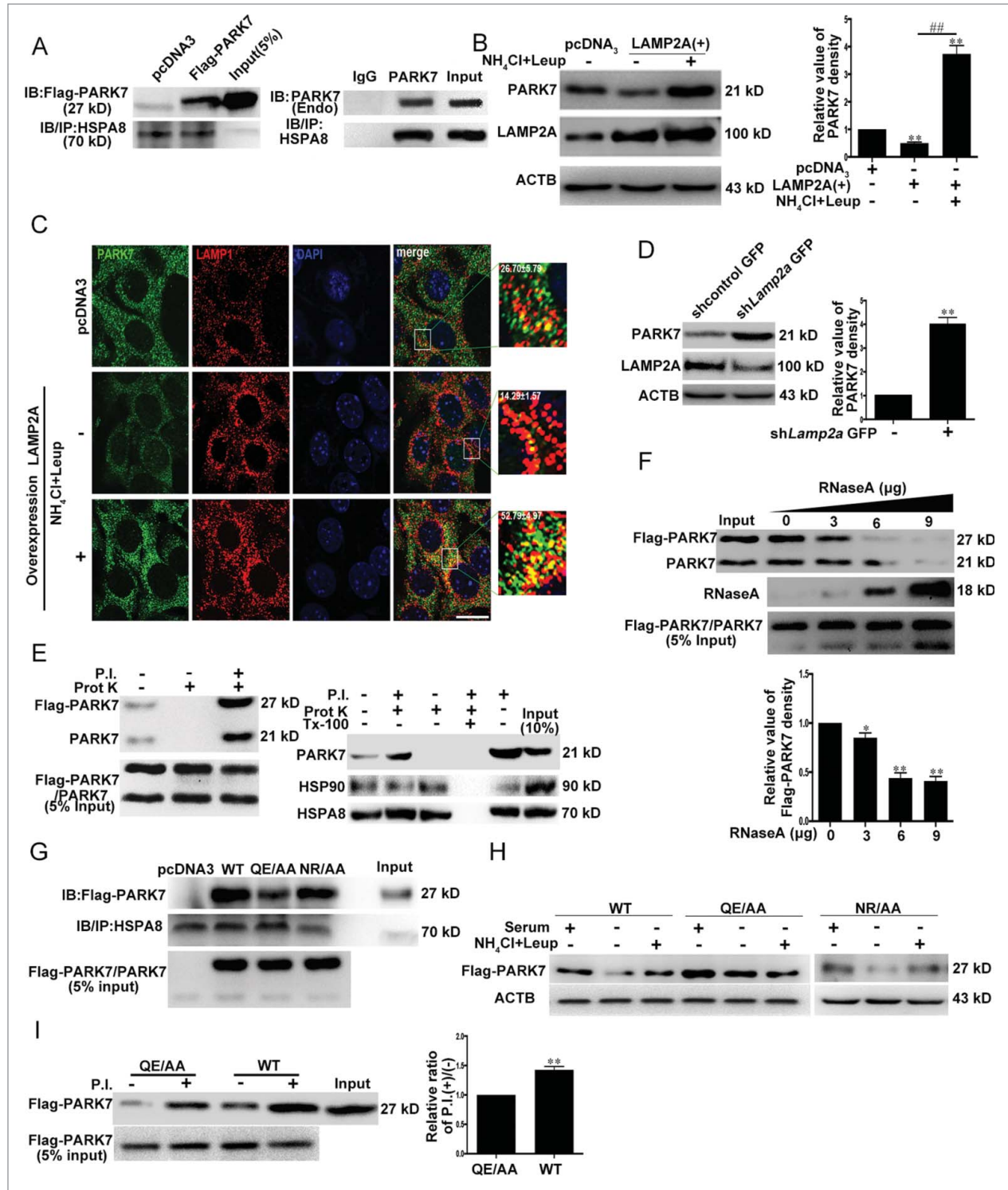

Figure 2. (For figure legend, see page 1219.)

cross-linking agent disuccinimidylsuberate (DSS) before immunoblotting. Modulating CMA activity by sh*Lamp2a* or starvation led to a clear change in the monomeric form of PARK7 without much effect on the level of dimer (Fig. 3F). Similarly, inhibition of lysosomal activity by NH_4Cl and leupeptin (Leup) for 18 h also increased the level of PARK7 monomer without altering the level of dimer (Fig. 3F). However, more prolonged inhibition of lysosomal activity led to a further increase in the level of PARK7 monomer and some increase in its dimer. Analysis of MPP^+ treated samples showed that compared to the slight change in the level of PARK7 dimer, MPP^+ caused a much greater reduction in the level of PARK7 monomer (Fig. 3G). Interestingly, reducing CMA activity by sh*Lamp2a* significantly attenuated MPP^+-induced degradation of monomeric PARK7. Thus, CMA appears to preferentially target the oxidatively damaged monomeric PARK7 for removal, and the extensive accumulation of the oxidized PARK7 monomer following a reduction of lysosomal and CMA activity affects the formation or alters the balance of PARK7 dimer.

Regulation of mitochondrial morphology and function by the CMA-PARK7 pathway under MPP^+ stress

Our data above showed clearly that LAMP2A-mediated CMA pathway directly regulates PARK7 homeostasis. Since PARK7 is known to be required for mitochondrial integrity,[35] we tested the possibility that CMA may protect mitochondria from stress-induced damage via PARK7. We knocked down LAMP2A in SN4741 cells using lentivirus expressing *Lamp2a* shRNA and showed that under basal conditions, there was no significant difference in the mitochondrial morphology assessed by MitoTracker Red between control and cells with the reduced LAMP2A (Fig. 4A). Under MPP^+-induced stress, cells with the reduced level of LAMP2A showed a much greater degree of mitochondrial fragmentation (Fig. 4A). To further demonstrate that CMA is required for maintaining mitochondrial function, we measured mitochondrial membrane potential (MMP) and ROS levels. Our data showed that although MMP levels were the same between sh*Lamp2a* and control cells under the basal condition, reduction of LAMP2A further exacerbated MPP^+-induced decrease in MMP (Fig. 4B). Interestingly, compared to mitochondrial morphology and MMP, the levels of ROS were significantly elevated in cells with the reduced level of LAMP2A even under the basal condition. Reducing the level of LAMP2A further exacerbated the MPP^+-induced increase in ROS (Fig. 4C). Together, these findings demonstrate that LAMP2A and CMA activity is required for maintaining mitochondrial homeostasis under stress. To assess if PARK7 functions downstream of CMA in maintaining mitochondrial integrity, we overexpressed PARK7, which significantly increased the level of functional dimer (Fig. S9A), in above studies and showed that increase of PARK7 significantly reduced the mitochondrial fragmentation and increased the appearance of longer mitochondrial tubules in cells treated with MPP^+ and sh*Lamp2a* (Fig. 4A). Similarly, overexpression of PARK7 also attenuated the MPP^+- or MPP^+ and sh*Lamp2a*-induced decrease of MMP (Fig. 4B), and reduced the level of ROS after LAMP2A knockdown and MPP^+ treatment (Fig. 4C). Consistent with the above data, increasing the level of LAMP2A protected mitochondria from MPP^+-induced fragmentation as evidenced by the appearance of longer mitochondrial tubules, partially restored MMP, and attenuated MPP^+-induced ROS production in SN4741 cells (Fig. 4D to F). However, silencing *Park7* (Fig. S9B) largely abrogated the protective effects of LAMP2A against MPP^+-induced stress (Fig. 4D to F). In support of this, overexpression of mutant QE→AA exacerbated MPP^+-induced decrease in MMP and production of ROS (Fig. 4G and H). Together, these data demonstrate clearly that CMA-PARK7 pathway plays a critical role in maintaining mitochondrial morphology and function under stress.

Inhibition of the CMA-PARK7 pathway in neurotoxin-induced cell death

Our previous studies showed that inhibition of CMA increased the sensitivity of cells to neurotoxic stress.[15] To evaluate the role of CMA-PARK7 pathway in neurotoxin-induced cell

Figure 2. (see previous page) Degradation of PARK7 by CMA. (A) Interaction between PARK7 and HSPA8. Left panel: lysates of HEK293 cells transfected with Flag-PARK7 were immunoprecipitated with an anti-HSPA8 antibody. The precipitates were immunoblotted for Flag-PARK7 with an anti-Flag antibody as shown. Right panel: the cytoplasmic fraction of SN4741 cells were immunoprecipitated with an anti-HSPA8 antibody (IgG lane indicates that a control IgG was used in the immunoprecipitation). The precipitates were immunoblotted for PARK7 with an anti-PARK7 antibody. (B) The effect of LAMP2A on PARK7. SN4741 cells were transfected with $pcDNA_3$ or a LAMP2A overexpression construct for 48 h in the absence or presence of NH_4Cl and leupeptin, and the levels of LAMP2A and PARK7 were determined by immunoblotting. Right graph shows the quantification of PARK7 (mean ± SEM, n = 3; **, $P < 0.01$ compared to the control group; ##, $P < 0.01$ compared to the indicated group). (C) The effect of upregulated LAMP2A on PARK7 and LAMP1 colocalization. SN4741 cells were treated as in (B). The colocalization of PARK7 and LAMP1 was determined by immunofluorescence. The magnified images were also provided. The ratio of colocalization was calculated. Scale bar: 50 μm. (D) The effect of reducing LAMP2A on PARK7. SN4741 cells were transfected with lentivirus expressing control or shRNA to *Lamp2a*. The levels of LAMP2A and PARK7 were determined by immunoblotting. The right graph shows the quantification of PARK7 (mean ± SEM, n = 3; **, $P < 0.01$ compared to the control group). (E) Lysosomal binding and uptake of PARK7. Left panel: the purified lysosomes with or without a cocktail of protease inhibitors (P.I.) were incubated with the lysates of HEK293 cells overexpressing PARK7 for 20 min at 37°C. At the end of the incubation, samples were treated with proteinase K (prot K; 50 μg/ml) for 10 min at 0°C. After washing, the presence of PARK7 was determined by immunoblotting. Left panel: the left lane corresponds to PARK7 associated with the lysosomes in the absence of P.I; the middle lane shows that proteinase K efficiently removes PARK7 bound to the lysosomal membrane; and the right lane indicates the total amount of PARK7 associated with lysosomes under the condition. Right panel: the purified lysosomes with or without a cocktail of protease inhibitors (P.I.) were incubated with the purified PARK7 for 20 min at 37°C and followed with or without proteinase K and/or Triton X-100 (Tx-100) treatment (10 min at 0°C). Levels of PARK7 and lysosomal HSP90 and HSPA8 were determined by immunoblotting. (F) The effect of a known CMA substrate RNase A on the association of PARK7 with lysosomes. The experiment was carried out as in (E) right panel with or without increasing concentrations of RNase A for 20 min at 37°C. The presence of PARK7 and RNase A was determined by immunoblotting. Lower graph shows the quantification of PARK7 associated with lysosomes (mean ± SEM, n = 3; *, $P < 0.05$; **, $P < 0.01$ compared to the control group). (G) Binding between HSPA8 and wild-type (WT) or mutated PARK7. Lysates of HEK293 cells transfected with wild-type (WT) and mutated (QE→AA or NR→AA) PARK7 were immunoprecipitated with an anti-HSPA8 antibody. The precipitates were immunoblotted for Flag-PARK7 with an anti-Flag antibody. The lower graph shows the quantification of Flag-PARK7 coimmunoprecipitated with HSPA8. (H) Degradation of PARK7 mutant QE→AA and NR→AA by serum deprivation. SN4741 cells transfected with the indicated plasmids were treated as described in Fig. 1B. (I) Interaction between PARK7 mutant QE/AA and lysosomes. The lysates expressing PARK7 WT or QE→AA were incubated with purified lysosomes as described in (E). The right graph shows the quantification of wild-type and mutated QE→AA Flag-PARK7 associated with lysosomes (mean ± SEM, n = 3; **, $P < 0.01$).
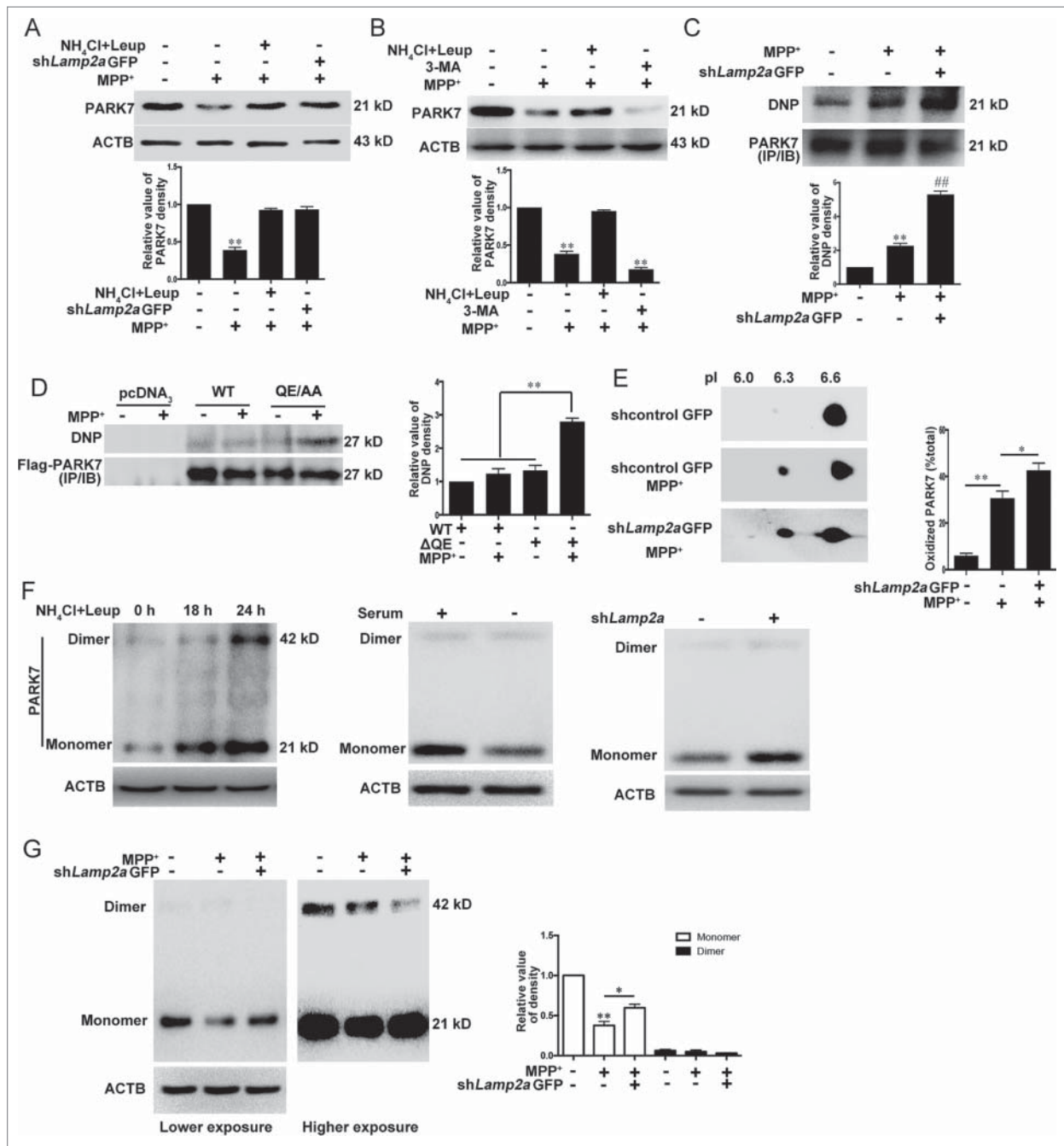
Figure 3. Degradation of oxidized and damaged PARK7, by CMA. (A) CMA-mediated degradation of PARK7 under MPP$^+$. SN4741 cells transfected with lentivirus expressing sh*Lamp2a* were treated with MPP$^+$ (50 μM) in the presence or absence of NH$_4$Cl and leupeptin (Leup) for 24 h and the levels of PARK7 were determined by immunoblotting. The lower graph shows the quantification of PARK7 levels (mean $\pm$ SEM, n = 3; **, $P < 0.01$ compared to the control group). (B) The effect of 3-MA on the MPP$^+$-induced decrease of PARK7 level. SN4741 cells were treated with 50 $\mu\mu$ MPP$^+$ and 10 mM 3-MA in the presence or absence of NH$_4$Cl and leupeptin. The levels of PARK7 were determined by immunoblotting. The lower graph shows the quantification of PARK7 levels (mean $\pm$ SEM, n = 4; **, $P < 0.01$ compared to the control group). (C) The effect of reducing LAMP2A on the level of carbonyl PARK7 following MPP$^+$ treatment. The lysates from SN4741 cells transfected with lentivirus expressing sh*Lamp2a* and treated with 50 $\mu\mu$ MPP$^+$ for 24 h were immunoprecipitated with an anti-PARK7 antibody. The levels of PARK7 and DNP-derivatized carbonyl groups were determined by immunoblotting. The lower graph shows the quantification of derivatized carbonyl groups levels (mean $\pm$ SEM, n = 4; ** and $^{##}$, $P < 0.01$ compared to the control group). (D) Increasing rate of carbonyl oxidation of PARK7 QE→AA mutant. SN4741 cells were transfected with the indicated plasmids, treated with 50 $\mu\mu$ MPP$^+$ for 12 h, and assayed as described in (C). The right graph shows the quantification of the levels of the derivatized carbonyl groups (mean $\pm$ SEM, n = 3, $^{**}P < 0.01$). #x2206;QE, QE→AA. (E) Accumulation of the acidic forms of PARK7 following knockdown of LAMP2A. SN4741 cells were treated as described in (A). The protein extracts were separated by 2D gel electrophoresis and analyzed for PARK7. The right graph shows the quantification of acidic form of PARK7 (mean $\pm$ SEM; n=3; *, $P < 0.05$; **, $P < 0.01$). (F) The effect of lysosomal and CMA activity on the PARK7 monomer and dimer. SN4741 cells were treated with NH$_4$Cl and Leupeptin (Leup) or serum deprivation for the indicated duration, or transfected with lentiviral sh*Lamp2a* and then treated with DSS (5 mM). The levels of PARK7 were detected by immunoblotting. (G) Degradation of monomeric form of PARK7 by CMA. Lysates from SN4741 cells treated as described in (A) and (F) were analyzed for the PARK7 monomer and dimer by immunoblotting. The right graph shows the quantification of the monomeric and dimeric forms of PARK7 (mean $\pm$ SEM, n = 4; **, $P < 0.01$ compared with the control group and *, $P < 0.05$ compared with the indicated group).
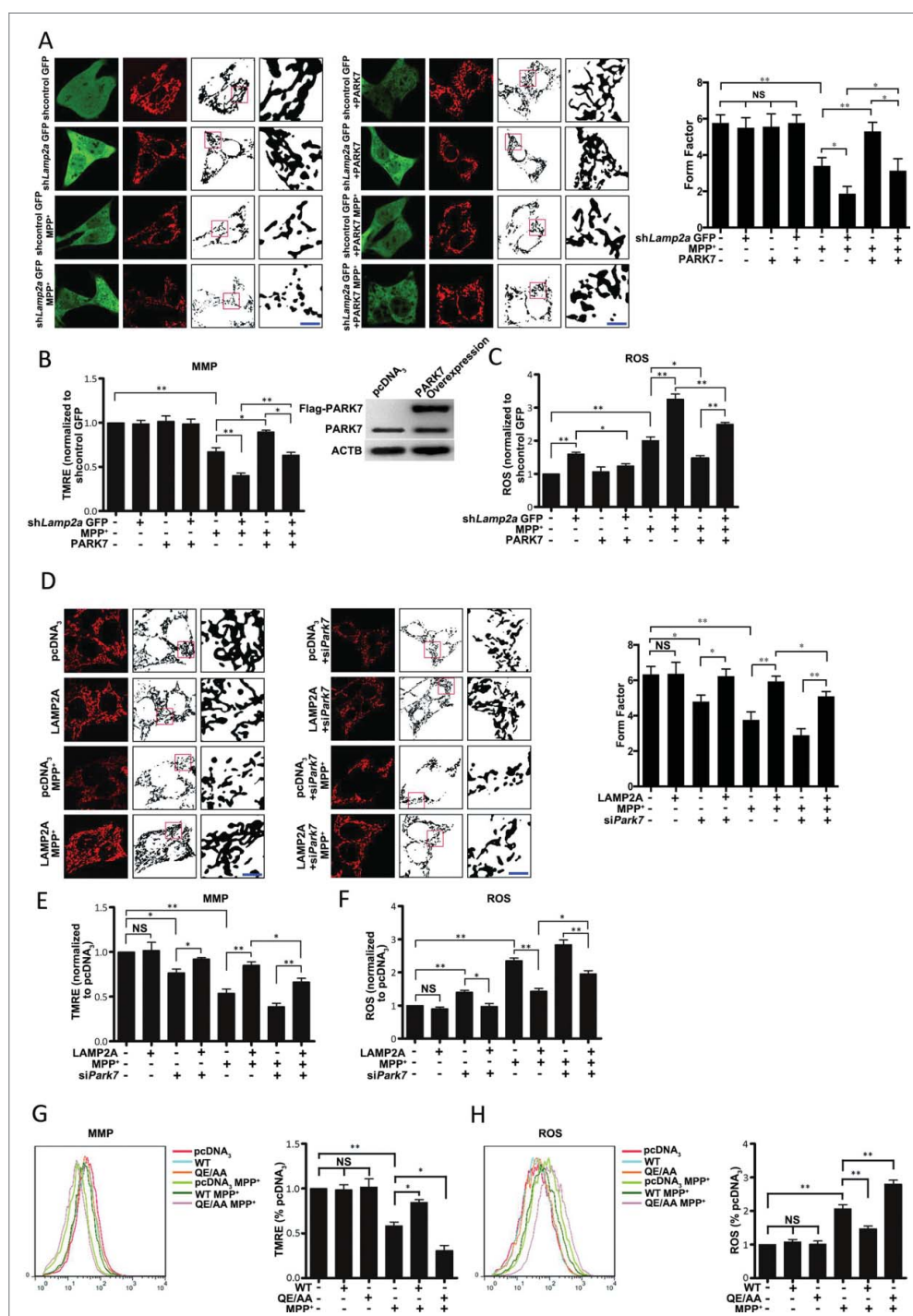
Figure 4. Regulation of mitochondria by CMA through PARK7. (Ato C) The effect of overexpression of PARK7 on sh*Lamp2A*- and MPP⁺-induced mitochondrial dysfunction. SN4741 cells transfected with control GFP or sh*Lamp2a-GFP* lentivirus were transfected with the control or PARK7 plasmids, treated with MPP⁺ (50 μM) for 24 h and analyzed (mean ± SEM; n = 3; *, $P < 0.05$; **, $P < 0.01$). For mitochondrial morphology, cells were stained with MitoTracker Red (10 nM) for 20 min at 33°C. Mitochondrial morphology in living SN4741 cells was analyzed by live-cell imaging (Nikon, C2 Si, Japan) (green, GFP; red, MitoTracker Red; insets represent boxed areas) using ImageJ 1.41 software (A). The right graph shows the form factor of mitochondria, which reflects the complexity and branching, calculated as (perimeter[2])/(4π·surface area). For MMP, cells were incubated with TMRE (200 nM) for 20 min at 33°C. Ten thousand cells were assayed for TMRE fluorescence by flow cytometry (B). For ROS levels, cells were incubated with CellROX→ Deep Red Reagent (2.5 $\mu\mu$). Ten thousand cells were assayed for CellROX→ Deep Red Reagent fluorescence by flow cytometry (C). Scale bar: 50 μm. (Dto F) The effect of downregulation of PARK7 on LAMP2A-induced protection of mitochondria. SN4741 cells transfected with the control or LAMP2A plasmid with or without siRNA oligonucleotides for *Park7* were treated with MPP⁺ (50 μM) for 24 h. Mitochondrial functions were assayed as described in (Ato C) (mean ± SEM; n = 3; *, $P < 0.05$; **, $P < 0.01$). Scale bar: 50 μm. (G and H) The effect of overexpressing PARK7 QE→AA on MMP (G) and ROS (H) under oxidative stress. SN4741 cells were transfected with the indicated plasmids and treated with MPP⁺ for 24 h. MMP and ROS were assayed as described as above. Right graphs show the quantifications (mean ± SEM; n = 3; *, $P < 0.05$; **, $P < 0.01$).

death, we infected SN4741 cells with lentivirus expressing *Lamp2a* shRNA (sh*Lamp2a*), treated cells with MPP[+] for 24 h, and measured cell death by TUNEL assay. sh*Lamp2a* alone did not cause significant death under basal condition while MPP[+] did. However, blocking CMA greatly increased the number of TUNEL cells compared to MPP[+] treatment alone (Fig. 5A). Overexpression of PARK7 clearly decreased the number of TUNEL staining under MPP[+] and sh*Lamp2a* conditions (Fig. 5A). These results were confirmed by measuring cellular viability with LDH (lactate dehydrogenase) (Fig. 5C). Conversely, increasing CMA by overexpression of LAMP2A protected cells from MPP[+]-induced death as determined in both TUNEL and LDH assays (Fig. 5B and D). Silencing *Park7* clearly attenuated LAMP2A-induced protection (Fig. 5B and D). Thus, dysfunction on CMA-PARK7 pathway may underlie the stress-induced loss of cellular viability.

Discussion

Mitochondria are an essential mediator of neuronal survival and death. Mitochondrial dysfunction and oxidative stress play a critical pathogenic role in neurodegenerative diseases, especially Parkinson disease.[2] Increasing evidence from PD patients, animal toxin models, and genetic models indicates that mitochondrial quality control including prevention of damage and cleaning of damaged mitochondria may be central to elucidating DA neuron death in PD. Damaged mitochondria in cells are removed by a specialized form of macroautophagy named mitophagy, a process important for mitochondrial homeostasis.[36] Interestingly, although autophagy is clearly needed as a protective mechanism for cells to depose damaged mitochondria, excessive autophagy activity appears to be detrimental to mitochondria. Uncontrolled mitophagy contributes to cellular stress by the mitochondrial biogenesis and hindering the overall mitochondrial function.[37] CMA and macroautophagy are linked. It is known that under stress conditions, a decrease in CMA can lead to a compensatory increase in macroautophagy.[38] However, whether and how CMA may be directly involved in protecting mitochondria from damage remained unknown. In this study, we provide evidence that CMA plays an essential role in maintaining mitochondrial integrity under stress. Our findings indicate that CMA activity is both necessary and sufficient for protecting mitochondrial morphology and function under stress, revealing an important role for CMA in protecting mitochondrial homeostasis. These data establish a direct regulatory link between autophagy and mitochondrial function.

Besides ubiquitin-proteasome system degrading proteins tagged with ubiquitin molecules, CMA is the most selective form of protein degradation process that specifically controls the removal of individual cytosolic proteins. Under stress, CMA is usually activated to selectively degrade nonfunctional or damaged proteins.[38] This has been proposed to prevent the accumulation of potentially toxic proteins and may underlie the process by which CMA maintains cellular homeostasis and survival under stress.

Our identification of PARK7 as the direct target mediating the mitochondrial protective effect of CMA is especially interesting. PARK7 is known to play a critical role in antioxidative defense and mitochondrial function. Its deficiency results in elevated ROS production and mitochondrial damage. Our data that CMA preferentially degrades nonfunctional extensively oxidatively damaged PARK7 under stress that provides a mechanistic explanation for its protective effect on mitochondria. Since the oxidatively damaged PARK7 have been confirmed as nonfunctional and their levels found to increase in the brain tissue of PD patients,[24] they raise the possibility that dysfunction of CMA-mediated degradation of PARK7 may contribute to the observed accumulation of nonfunctional PARK7 in PD. Conditions that impair CMA such as aging or genetic factors may, therefore, be partially responsible for accumulation of damaged PARK7 in PD.[39] Consistent with this notion, the level of carbonyl oxidation of mutant QE→AA, which is resistant to degradation by CMA, increases in SN4741 cells exposed to MPP[+]. Our results showed that MPP[+] treatment increased the level of the more acidic form of PARK7. Many studies have demonstrated that MPTP or MPP[+] causes oxidative stress, including carbonyl and other forms of protein oxidation.[40-43] Oxidative stress correlates with a shift of pI of PARK7 to be more acidic.[33] Our recent studies have shown that oxidative stress-induced carbonyl oxidation of MEF2D correlates with its migration to the acidic range.[15] Taken together, these findings suggest that carbonyl oxidation of PARK7 may be responsible for its migration to the acidic range. Since oxidized PARK7 is removed by CMA, the increased level of the acidic PARK7 observed after oxidative stress may at least in part reflect a certain degree of loss of CMA activity.

One of the early key steps in the CMA process is the highly efficient and specific recognition of substrates by chaperone protein HSPA8.[44] This specificity is largely achieved via the interaction between HSPA8 and the conserved KFERQ-like motif found in the substrate proteins. The key features of this motif are the presence of multiple charged amino acid residues that are either preceded or followed by a glutamine. It has been proposed that due to their structure similarity, an asparagine residue may, under certain conditions, substitute the function of glutamine in constituting such a motif.[29] Based on these criteria, we analyzed PARK7 protein sequence and identified 2 canonical CMA recognition motifs and one imperfect motif. Using mutagenesis approach, we ruled out the involvement of the motif starting with N144. Our further analysis showed that mutation of Q95E to AA (QE→AA) clearly reduced the degradation of PARK7 by CMA. These data are certainly consistent with the prediction of I[91]LKEQ[95] being the strongest motif responsible for CMA targeting. Interestingly, QE→AA mutant did not lose entirely its interaction with HSPA8 by co-immunoprecipitation assay. There are several possibilities for this. First, it is possible that there may be other CMA targeting motifs in PARK7. They may play a minor role in mediating the regulation of PARK7 by CMA. Second, it is possible that mutation of Q95 may alter the structure of PARK7 in such a way that allows the exposure of motifs that are normally hidden so that they can be recognized by HSPA8. These 2 possibilities are not mutually exclusive. Finally, the residual interaction detected between HSPA8 and PARK7 QE→AA mutant simply reflects a background signal in our assay. Further experiments are needed to delineate these possibilities.

Dysfunction of CMA activity has been implicated in PD pathogenesis by several studies. First, several risk factors associate
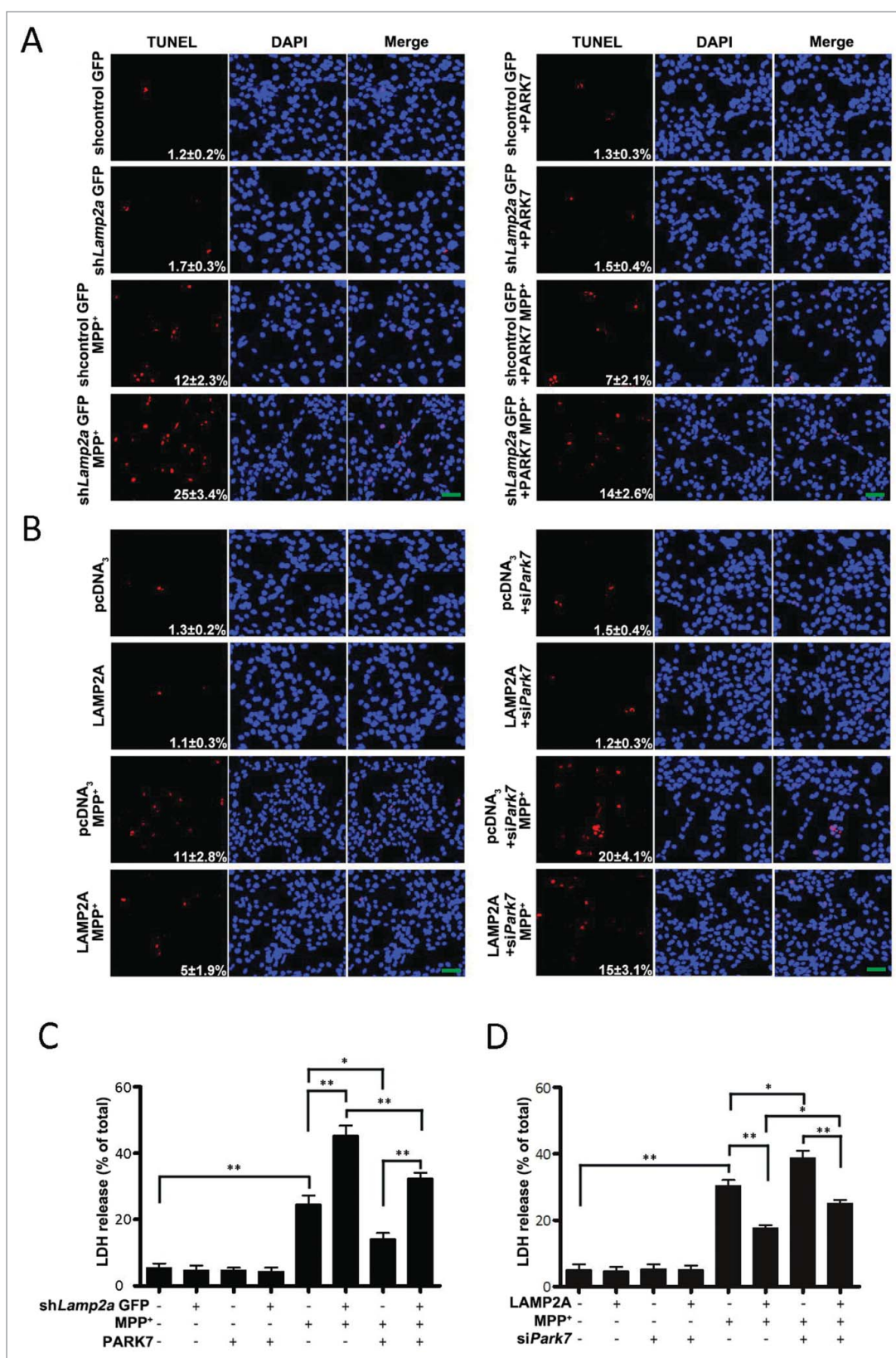
Figure 5. Modulation of the SN4741 cell viability by the CMA-PARK7 pathway. (A and B) The effect of modulating LAMP2A or PARK7 on MPP$^+$-induced cellular apoptosis by TUNEL. SN4741 cells treated as in Fig. 4A or 4D were stained for TUNEL (mean ± SEM; n = 3). The numbers in the TUNEL panels indicate the ratio of TUNEL-positive cells/total cells. Scale bar: 100 μm. (C and D) The effect of modulating LAMP2A or PARK7 on MPP$^+$-induced cell death by LDH release assay. SN4741 cells treated as described in (A and B) were assessed for cytotoxicity by LDH release assay (mean ± SEM; n = 3; *, $P < 0.05$; **, $P < 0.01$).

with neurodegenerative disorders including PD clearly affect CMA. In addition to oxidative stress, both aging, the biggest risk factor for PD, and neurotoxins are associated with changes in CMA.[45,46] Second, CMA has been shown to directly modulate neuronal survival machinery. For example, transcription factor MEF2D is a critical regulator of neuronal viability.[47-49] Loss of MEF2 activity contributes to DA neuronal death in PD models.[50] CMA has been shown to directly remove damaged MEF2D to maintain its function.[14,15] Inhibition of CMA by SNCA contributes to dysregulation of MEF2D homeostasis and underlie neuronal vulnerability to stress.[14] Third, there appears to be a particularly strong link between familial PD and CMA. Mutations of *SNCA, LRRK2,* and *UCHL1* genes cause familial PD.[51-53] Both LRRK2 and SNCA are themselves CMA substrates, whose normal turnover requires adequate CMA activity.[10,11,54] Moreover, pathogenic mutants of all 3 proteins significantly attenuate the CMA process.[45,46] Together with the findings presented in this study, these results suggest that CMA is a point at which multiple PD-associated pathological factors converge their toxic activity. Since the CMA substrate MEF2D directly regulates mitochondrial complex I activity,[44] our data indicate that CMA and mitochondria are linked through multiple pathways, which is much more critical and complex than previously appreciated, especially under stress and in pathological conditions such as PD.

Materials and methods

Plasmids, antibodies and chemicals

The LAMP2A construct was a gift from Dr. Zixu Mao (Departments of Pharmacology and Neurology, School of Medicine, Emory University). *Lamp2a* shRNA (sh*Lamp2a*)-expressing lentivirus (target sequence 1: 5′-GCGTTTCAGATCAACACCTTT-3′; target sequence 2: 5′-GCAGAATGGGAGATGAATTTC-3′; target sequence 3: 5′-CCGTTGGAAACTACAGCATTA-3′) and a nonsilencing sequence-expressing lentivirus (5′-TTCTCCGAACGTGTCACGT-3′) were supplied commercially by Neuron Biotech Co. Ltd. (Shanghai, China). The FLAG-tagged human PARK7 construct was kindly provided by H. Ariga (Hokkaido University, Japan). The following antibodies were used: anti-PARK7 (Abcam, ab76008), anti-HSPA8 (Abcam, ab19136), anti-ACTB (Abcam, ab8226), anti-LAMP1 (Abcam, ab13523), anti-LAMP2A (Abcam, ab125068), anti-Flag (Abcam, 1162), anti-SQSTM1 (Abcam, ab56416), anti-MAP1LC3B (Sigma, L7543). MPP$^+$ (D048), NH$_4$Cl (A9434), MG132 (C2211), 3-MA (M9281)#xff0c; RNase A (R6513), proteinase K (P2308) were purchased from Sigma; TMRE (T669), CellROX→ Deep Red Reagent (C10422) and CM-H2DCFDA (C6827) from Life Technologies; the OxyBlot protein oxidation detection kit (S7150) from Chemicon International; the Cytotoxicity LDH Detection Kit (04744926001) from Roche; protein A/G PLUS-Agarose (sc2003) from Santa Cruz Biotechnology; and ReadyPrep^{TM} 2-D Starter Kit (1632105) from Bio-Rad. All the other chemicals were obtained from the Sigma-Aldrich company unless otherwise stated.

Cell culture and plasmid transfection

SN4741 cells were cultured at 33°C with 5% CO$_2$ in Dulbecco's modified Eagle's medium supplemented with 10% fetal bovine serum, 1% glucose, 100 U/ml penicillin-streptomycin, and L-glutamine.[55] The human embryonic kidney (HEK) 293 cells were maintained in DMEM supplemented with 10% fetal bovine serum, 2 mM L-glutamine, and 100 U/ml penicillin-streptomycin. To remove the serum, cells were washed 3 times with phosphate-buffered saline (PBS; Sigma, P5493) and placed in serum-free medium. For live-cell imaging, cells were grown in a confocal Petri dish (NEST, 801001). Cells were transfected with expression plasmids or RNA oligonucleotides using Lipofectamine 2000 reagent (Invitrogen, 11668019) according to the manufacturer's instructions.

Western blot analysis

Cells were washed 3 times with ice-cold PBS, scraped in cold PBS, collected by centrifugation at 300 × g, then incubated in a lysis buffer (50 mM Tris-HCl, 150 mM NaCl, 1.0 mM EDTA, 0.1% Triton-X100 [Sigma, X100], protease and phosphatase inhibitors [abcam, ab201119]) for 30 min on the ice. Lysates were sonicated for 5 s 3 times and centrifuged at 13000 × g for 10 min. The supernatant fractions were collected and determined for the protein concentration by using the BCA assay (Beyotime, P0010). The following antibodies for western blot were used: anti-PARK7, anti-ACTB, anti-LAMP2A, anti-HSPA8, and anti-LAMP1.

Coimmunoprecipitation assay

HEK293 cells were transfected with Flag-tagged pcDNA$_3$ or wild-type PARK7. After 48 h, cells were collected as mentioned above. The supernatant fractions were precleared with protein A/G PLUS-agarose and immunoprecipitated with rat anti-HSPA8 antibody overnight at 4°C. The lysate and antibody (immunocomplex) solution were transferred to the tube containing the Protein A/G PLUS-Agarose, followed by incubating with gentle rocking for 4 h at 4°C. Immunoprecipitated proteins were collected by centrifugation at 1000 × g for 2 min followed by 3 washes of the pellet with cell lysis buffer. Immunoprecipitated proteins were eluted from beads by heating in the presence of Laemmli sample buffer and analyzed by western blotting using anti-Flag antibody.

Isolation of lysosomes

Lysosomes were isolated as described previously. Briefly, male Sprague-Dawley rats (200 to 250 g) were fasted for 20 h and then were sacrificed via anesthetic overdose (CO$_2$). Livers were removed and homogenized in the extraction buffer (Sigma, lysosome isolation kit, LYSISO1). Lysosomes were isolated from a light mitochondrial-lysosomal fraction and tested for LAMP1 levels by immunoblotting. Lysosomal integrity was assessed using the dye Neutral Red (Sigma, N7005).

Binding and uptake by lysosomes

The assays were carried out as described previously.[56] Freshly isolated intact lysosomes were pretreated with or without the protease inhibitor cocktail (abcam, ab65621) and then were incubated with a lysate prepared from HEK293 cells overexpressing

wild-type PARK7 in MOPS buffer (10 mM 3-[N-morpholino] propanesulfonic acid, pH 7.3, 0.3 M sucrose [Amresco, 0670]) for 20 min at 37°C. After the incubation, all samples were centrifuged at 16,100 × g (Eppendorf centrifuge, 5415R, Germany) for 5 min at 4°C, and the pellet fractions were washed 3 times with 100 μl of cold incubation buffer. The final pellet fractions were resuspended in Laemmli buffer, subjected to SDS-PAGE and immunoblotted with anti-PARK7 antibody. In the presence or absence of inhibitor of lysosomal proteases, the protein detected correlates to either the amount of protein both bound to the lysosomal membrane and taken up by lysosomes or the amount of protein bound to the lysosomal membrane, respectively.

Quantitative real-time PCR (qrtPCR)

Total RNA was extracted according to the manufacturer's protocol for TRIzol Reagent (Invitrogen, 15596026). RNA (1 μg) was reversely transcribed using Brilliant II SYBR green single-step quantitative RT-PCR master mix (Stratagene, 600825). Real-time quantitative RT-PCR (qRT-PCR) was performed using an Mx3005 or Mx4000 multiplex quantitative PCR system (Stratagene, Santa Clara, CA). Quantification of mRNA was performed using Brilliant II SYBR green single-step quantitative RT-PCR master mix with 10 ng of total RNA in 25 μl reaction mixtures. The thermal profile was 50°C for 30 min, 95°C for 15 min, and then 40 cycles of 95°C for 30 s and 55°C for 30 s. Fluorescence was measured at the end of the 55°C step during every cycle. Primer sequences as follow: *Park7* forward, 5′-GAGGTTCCTGCGGACTAGC-3′; *Park7* reverse, 5′-TATGAGGCCCTTCCTGCTCT-3′; *Actb* forward, 5′-AAG-GACTCCTATAGTGGGTGACGA-3′; *Actb* reverse, 5′-ATCTTCTCCATGTCGTCCCAGTTG-3′.

Site-directed mutagenesis of PARK7

Site-directed mutagenesis was performed using the QuikChange Lightning Site-directed Mutagenesis Kit (Stratagene, 210518) according to the manufacturer's instructions. The wild-type plasmid encoding human PARK7 was used as a template in the mutagenesis reaction. The mutagenic oligonucleotides designed to produce the desired point mutations were as follows: QE→AA, forward, 5′-GTGAAGGAGATACTGAAGGAGGCTGCTAACCGGAAGGGCCTGATAGCC-3′; QE→AA reverse, 5′-GGCTATCAGGCCCTTCCGGTTAGCAGCCTCCTTCAGTATCTCCTTCAC-3′; NR→AA, 5′-CGGCTTGTAAGAATCAGGCCGTCAGC AGCCACACGATTCTCAGAGTAGGTGT-3′; NR→AA, 5′-ACACC-TACTCTGAGAATCGTGTGGCTGCTGACGGCCTG ATTCT-TACAAGCCG-3′. Plasmids containing the desired mutations were transformed into XL10-Gold Ultracompetent cells (Stratagene, 200315). All mutated sequences were confirmed by sequencing both strands of the construct.

Protein oxidation detection

Protein oxidation was determined using the OxyBlot protein oxidation detection kit (Millipore, S7150) according to the manufacturer's instructions. Briefly, the lysates from SN4741 cells transduced with a lentivirus expressing shLamp2a and treated with 50 $\mu\mu$ MPP$^+$ for 24 h were immunoprecipitated with anti-PARK7 antibody. The samples were denatured by adding 12% SDS (Sigma, 74255), derivatized by adding 1 × DNPH solution (Millipore, S7150), incubated at room temperature for 15 min, and neutralized with neutralization solution (Millipore, S7150) and 2-mercaptoethanol (Millipore, S7150) at a final concentration of 0.74 M. The levels of DNP were detected using immunoblotting.

2D gel electrophoresis

The lysates of cells (150 μg) were resuspended in a rehydration buffer (Bio-Rad, ReadyPrep^{TM} 2-D Starter Kit) at a final concentration of 2 to 4 mg/ml. Samples were separated using an isoelectric-focusing phoresis gel (pH 5 to 8). The first-dimension gels were subsequently separated on 10% Tris-HCl SDS-PAGE gels, and the levels of PARK7 were detected using western blotting. 2D SDS-PAGE standards (Bio-Rad, 1610320) were used to calibrate pI and molecular weights.

Cross-linking assay

Cells were washed 3 times with ice-cold PBS, scraped in cold PBS and incubated with 5 mM DSS (Pierce, 21555) for 30 min at room temperature. The reaction was quenched by incubation with 20 mM Tris-HCl, pH 7.5, for 15 min at room temperature. Lysates were analyzed by western blotting with anti-PARK7 antibody.

Mitochondrial staining

Mitochondrial staining was carried as per the manufacturer's instructions. Briefly, cells were plated into a confocal Petri dish (NEST 801001). After treatment, they were stained for 20 min with 10 nM MitoTracker Red CMXRos (Life Technologies, M7512) at 33°C. Mitochondria were imaged using a laser scanning confocal microscope (Nikon, C2 Si, Japan). Quantification of mitochondria morphology was performed as described previously.[57]

ROS detection

ROS production was measured by CellROX→ Deep Red Reagent (Life Technologies, C10422) or CM-H2DCFDA (Green) (Life Technologies, C6827) after lentivirus transduction or plasmid transfection, respectively. Cells transduced with lentivirus or transfected with plasmids were plated in 6-well plates. After treatment with 50 $\mu\mu$ MPP$^+$ for 24 h, cells were incubated with prewarmed PBS containing the probe for a final working concentration of 5 $\mu\mu$ dye for 30 min at 33°C. Following 3 washes with prewarmed PBS at 33°C to remove excess dye, cells were collected and resuspended in PBS. ROS generation was analyzed by flow cytometry (BD FACSCanto II, BD Biosciences, Piscataway, NJ, USA).

Mitochondrial membrane potential assay

Cells were treated as described above and incubated with TMRE (200 nM) for 20 min at 33°C. Following 3 washes with prewarmed PBS to remove excess TMRE, cells were collected

and resuspended in PBS. Analysis of mitochondrial membrane potential was performed using a flow cytometer (BD FACS-Canto II, BD Biosciences, Piscataway, NJ, USA). All the results were analyzed using Flowjo 7.6.1 software.

TUNEL staining

The terminal deoxynucleotidyl transferase dUTP nick end labeling (TUNEL) assay was performed with the One Step TUNEL Apoptosis Kit (Beyotime, JS, C1090). SN4741 cells were seeded onto chamber slides, transfected with plasmids and treated with MPP^+ (50 $\mu\mu$) for 24 h. Then cells were fixed, permeabilized, and incubated with TUNEL reaction mixture at 37°C for 1 h as described in the manufacturer's protocol. After washing twice with PBS (pH 7.4), slides were stained with DAPI (Sigma, D9542) and observed under a laser scanning confocal microscope (Nikon, C2 Si).

Measurement of cytotoxicity

Measurement of cytotoxicity was carried out using an LDH detection kit (Roche, 11644793001). Medium from individual wells was collected and incubated with a reaction mixture at 25°C for 30 min followed by the addition of a stop solution. The absorbance was measured at 490 nm using a SpectraMax M2 diagnostic microplate reader (Molecular Devices, Sunnyvale, CA, USA).

Statistical analysis

Statistical differences between group means were compared using one-way ANOVA, and analysis followed, in cases where a Bonferroni test was obtained (GraphPad PRISM 5.0 software). All values were expressed as mean ± SEM. A value of $P < 0.05$ was considered statistically significant.

Abbreviations

3-MA	3-methyladenine
CMA	chaperone-mediated autophagy
GFP	green fluorescent protein
HSPA8	heat shock protein 8
LAMP1	lysosomal-associated membrane protein 1
LAMP2A	lysosomal-associated membrane protein 2A
LDH	lactate dehydrogenase
Leup	leupeptin
LRRK2	leucine-rich repeat kinase 2
MAP1LC3B	microtubule-associated protein 1 light chain 3 β
MEF2D	myocyte enhancer factor 2D
MMP	mitochondrial membrane potential
MPP^+	1-methyl-4-phenylpyridinium
NH_4Cl	Ammonium chloride
PARK7	Parkinson disease (autosomal recessive, early onset) 7
PD	Parkinson disease
ROS	reactive oxygen species
SNCA	synuclein, α
SQSTM1	sequestosome 1
TUNEL	terminal deoxynucleotidyl transferase dUTP nick end labeling
Ub	ubiquitin
WT	wild type

References

[1] Fearnley JM, Lees AJ. Ageing and Parkinson's disease: substantia nigra regional selectivity. Brain 1991; 114:2283-301; PMID:1933245; http://dx.doi.org/10.1093/brain/114.5.2283

[2] Henchcliffe C, Beal MF. Mitochondrial biology and oxidative stress in Parkinson disease pathogenesis. Nat Clin Pract Neurol 2008; 4:600-9; PMID:18978800; http://dx.doi.org/10.1038/ncpneuro0924

[3] Balch WE, Morimoto RI, Dillin A, Kelly JW. Adapting proteostasis for disease intervention. Science 2008; 319:916-9; PMID:18276881; http://dx.doi.org/10.1126/science.1141448

[4] Komatsu M, Waguri S, Chiba T, Murata S, Iwata J-i, Tanida I, Ueno T, Koike M, Uchiyama Y, Kominami E, et al. Loss of autophagy in the central nervous system causes neurodegeneration in mice. Nature 2006; 441:880-4; PMID:16625205; http://dx.doi.org/10.1038/nature04723

[5] He L-q, Lu J-h, Yue Z-y. Autophagy in ageing and ageing-associated diseases. Acta Pharmacol Sin 2013; 34:605-11; PMID:23416930; http://dx.doi.org/10.1038/aps.2012.188

[6] Dehay B, Martinez−Vicente M, Caldwell GA, Caldwell KA, Yue Z, Cookson MR, Klein C, Vila M, Bezard E. Lysosomal impairment in Parkinson's disease. Movement Disord 2013; 28:725-32; PMID:23580333; http://dx.doi.org/10.1002/mds.25462

[7] Trinh J, Farrer M. Advances in the genetics of Parkinson disease. Nat Rev Neurol 2013; 9:445-54; PMID:23857047; http://dx.doi.org/10.1038/nrneurol.2013.132

[8] Dice JF. Chaperone-mediated autophagy. Autophagy 2007; 3:295-9; PMID:17404494; http://dx.doi.org/10.4161/auto.4144

[9] Velseboer DC, de Haan RJ, Wieling W, Goldstein DS, de Bie RM. Prevalence of orthostatic hypotension in Parkinson's disease: a systematic review and meta-analysis. Parkinsonism Relat Disord 2011; 17:724-9; PMID:21571570; http://dx.doi.org/10.1016/j.parkreldis.2011.04.016

[10] Cuervo AM, Stefanis L, Fredenburg R, Lansbury PT, Sulzer D. Impaired degradation of mutant α-synuclein by chaperone-mediated autophagy. Science 2004; 305:1292-5; PMID:15333840; http://dx.doi.org/10.1126/science.1101738

[11] Orenstein SJ, Kuo S-H, Tasset I, Arias E, Koga H, Fernandez-Carasa I, Cortes E, Honig LS, Dauer W, Consiglio A, et al. Interplay of LRRK2 with chaperone-mediated autophagy. Nat Neurosci 2013; 16:394-406; PMID:23455607; http://dx.doi.org/10.1038/nn.3350

[12] Kabuta T, Furuta A, Aoki S, Furuta K, Wada K. Aberrant interaction between Parkinson disease-associated mutant UCH-L1 and the lysosomal receptor for chaperone-mediated autophagy. J Biol Chem

2008; 283:23731-8; PMID:18550537; http://dx.doi.org/10.1074/jbc.M801918200

[13] Kabuta T, Wada K. Insights into links between familial and sporadic Parkinson's disease: physical relationship between UCH-L1 variants and chaperone-mediated autophagy. Autophagy 2008; 4:827-9; PMID:18635949; http://dx.doi.org/10.4161/auto.6560

[14] Yang Q, She H, Gearing M, Colla E, Lee M, Shacka JJ, Mao Z. Regulation of neuronal survival factor MEF2D by chaperone-mediated autophagy. Science 2009; 323:124-7; PMID:19119233; http://dx.doi.org/10.1126/science.1166088

[15] Gao L, She H, Li W, Zeng J, Zhu J, Jones DP, Mao Z, Gao G, Yang Q. Oxidation of survival factor MEF2D in neuronal death and Parkinson's disease. Antioxid Redox Signal 2014; 20:2936-48; PMID:24219011; http://dx.doi.org/10.1089/ars.2013.5399

[16] Wang B, Cai Z, Lu F, Li C, Zhu X, Su L, Gao G, Yang Q. Destabilization of survival factor MEF2D mRNA by neurotoxin in models of Parkinson's disease. J Neurochem 2014; 130:720-8; PMID:24848448; http://dx.doi.org/10.1111/jnc.12765

[17] Alvarez-Erviti L, Rodriguez-Oroz MC, Cooper JM, Caballero C, Ferrer I, Obeso JA, Schapira AH. Chaperone-mediated autophagy markers in Parkinson disease brains. Arch Neurol-chicago 2010; 67:1464-72; PMID:20697033; http://dx.doi.org/10.1001/archneurol.2010.198

[18] Wilson MA, Collins JL, Hod Y, Ringe D, Petsko GA. The 1.1-Å resolution crystal structure of DJ-1, the protein mutated in autosomal recessive early onset Parkinson's disease. Proc Natl Acad Sci U S A 2003; 100:9256-61; PMID:12855764; http://dx.doi.org/10.1073/pnas.1133288100

[19] Kahle PJ, Waak J, Gasser T. DJ-1 and prevention of oxidative stress in Parkinson's disease and other age-related disorders. Free Radical Bio Med 2009; 47:1354-61; PMID:19686841; http://dx.doi.org/10.1016/j.freeradbiomed.2009.08.003

[20] McCoy MK, Cookson MR. DJ-1 regulation of mitochondrial function and autophagy through oxidative stress. Autophagy 2011; 7:531-2; PMID:21317550

[21] Miller-Fleming L, Antas P, Pais TF, Smalley JL, Giorgini F, Outeiro TF. Yeast DJ-1 superfamily members are required for diauxic-shift reprogramming and cell survival in stationary phase. Proc Natl Acad Sci U S A 2014; 111:7012-7; PMID:24706893; http://dx.doi.org/10.1073/pnas.1319221111

[22] Miller DW, Ahmad R, Hague S, Baptista MJ, Canet-Aviles R, McLendon C, Carter DM, Zhu PP, Stadler J, Chandran J, et al. L166P mutant DJ-1, causative for recessive Parkinson's disease, is degraded through the ubiquitin-proteasome system. J Biol Chem 2003; 278:36588-95; PMID:12851414; http://dx.doi.org/10.1074/jbc.M304272200

[23] Bonifati V, Rizzu P, van Baren MJ, Schaap O, Breedveld GJ, Krieger E, Dekker MC, Squitieri F, Ibanez P, Joosse M, et al. Mutations in the DJ-1 gene associated with autosomal recessive early-onset parkinsonism. Science 2003; 299:256-9; PMID:12446870; http://dx.doi.org/10.1126/science.1077209

[24] Choi J, Sullards MC, Olzmann JA, Rees HD, Weintraub ST, Bostwick DE, Gearing M, Levey AI, Chin LS, Li L. Oxidative damage of DJ-1 is linked to sporadic Parkinson and Alzheimer diseases. J Biol Chem 2006; 281:10816-24; PMID:16517609; http://dx.doi.org/10.1074/jbc.M509079200

[25] Irrcher I, Aleyasin H, Seifert EL, Hewitt SJ, Chhabra S, Phillips M, Lutz AK, Rousseaux MW, Bevilacqua L, Jahani-Asl A, et al. Loss of the Parkinson's disease-linked gene DJ-1 perturbs mitochondrial dynamics. Hum Mol Genet 2010; 19:3734-46; PMID:20639397; http://dx.doi.org/10.1093/hmg/ddq288

[26] Moore DJ, Zhang L, Troncoso J, Lee MK, Hattori N, Mizuno Y, Dawson TM, Dawson VL. Association of DJ-1 and parkin mediated by pathogenic DJ-1 mutations and oxidative stress. Hum Mol Genet 2005; 14:71-84; PMID:15525661; http://dx.doi.org/10.1093/hmg/ddi007

[27] Son JH, Chun HS, Joh TH, Cho S, Conti B, Lee JW. Neuroprotection and neuronal differentiation studies using substantia nigra dopaminergic cells derived from transgenic mouse embryos. J Neurosci 1999; 19:10-20; PMID:9870933

[28] Fuertes G, Martindellano J, Villarroya A, Rivett A, Knecht E. Changes in the proteolytic activities of proteasomes and lysosomes in human fibroblasts produced by serum withdrawal, amino-acid deprivation and confluent conditions. Biochem j 2003; 375:75-86; PMID:12841850; http://dx.doi.org/10.1042/bj20030282

[29] Majeski AE, Dice JF. Mechanisms of chaperone-mediated autophagy. Int J Biochem Cell Biol 2004; 36:2435-44; PMID:15325583; http://dx.doi.org/10.1016/j.biocel.2004.02.013

[30] Bandyopadhyay U, Cuervo AM. Entering the lysosome through a transient gate by chaperone-mediated autophagy. Autophagy 2008; 4:1101-3; PMID:18927485; http://dx.doi.org/10.4161/auto.7150

[31] Cuervo AM, Dice JF. A receptor for the selective uptake and degradation of proteins by lysosomes. Science 1996; 273:501-3; PMID:8662539; http://dx.doi.org/10.1126/science.273.5274.501

[32] Meulener MC, Xu K, Thomson L, Ischiropoulos H, Bonini NM. Mutational analysis of DJ-1 in Drosophila implicates functional inactivation by oxidative damage and aging. Proc Natl Acad Sci U S A 2006; 103:12517-22; PMID:16894167; http://dx.doi.org/10.1073/pnas.0601891103

[33] Robert G, Puissant A, Dufies M, Marchetti S, Jacquel A, Cluzeau T, Colosetti P, Belhacene N, Kahle P, Da Costa CA, et al. The caspase 6 derived N-terminal fragment of DJ-1 promotes apoptosis via increased ROS production. Cell Death Differ 2012; 19:1769-78; PMID:22555455; http://dx.doi.org/10.1038/cdd.2012.55

[34] Hulleman JD, Mirzaei H, Guigard E, Taylor KL, Ray SS, Kay CM, Regnier FE, Rochet JC. Destabilization of DJ-1 by familial substitution and oxidative modifications: implications for Parkinson's disease. Biochemistry-us 2007; 46:5776-89; PMID:17451229; http://dx.doi.org/10.1021/bi7001778

[35] Irrcher I, Aleyasin H, Seifert E, Hewitt S, Chhabra S, Phillips M, Lutz AK, Rousseaux MW, Bevilacqua L, Jahani-Asl A, et al. Loss of the Parkinson's disease-linked gene DJ-1 perturbs mitochondrial dynamics. Hum Mol Genet 2010; 19:3734-46; PMID:20639397; http://dx.doi.org/10.1093/hmg/ddq288

[36] Chen H, Chan DC. Mitochondrial dynamics–fusion, fission, movement, and mitophagy–in neurodegenerative diseases. Hum Mol Genet 2009; 18:R169-R76; PMID:19808793; http://dx.doi.org/10.1093/hmg/ddp326

[37] Zhu JH, Gusdon AM, Cimen H, Van Houten B, Koc E, Chu CT. Impaired mitochondrial biogenesis contributes to depletion of functional mitochondria in chronic MPP+ toxicity: dual roles for ERK1/2. Cell Death Dis 2012; 3:e312; PMID:22622131; http://dx.doi.org/10.1038/cddis.2012.46

[38] Kiffin R, Christian C, Knecht E, Cuervo AM. Activation of chaperone-mediated autophagy during oxidative stress. Mol Biol Cell 2004; 15:4829-40; PMID:15331765; http://dx.doi.org/10.1091/mbc.E04-06-0477

[39] Cuervo AM, Wong E. Chaperone-mediated autophagy: roles in disease and aging. Cell Res 2014; 24:92-104; PMID:24281265; http://dx.doi.org/10.1038/cr.2013.153

[40] Rubio-Osornio M, Gorostieta-Salas E, Montes S, Pérez-Severiano F, Rubio C, Gómez C, Ríos C, Guevara J. Epicatechin Reduces Striatal MPP+-Induced Damage in Rats through Slight Increases in SOD-Cu, Zn Activity. Oxid Med Cell Longev 2015; 2015; PMID:26301040; http://dx.doi.org/10.1155/2015/276039

[41] Titze-de-Almeida SS, Lustosa CF, Horst CH, Del Bel E, Titze-de-Almeida R. Interferon Gamma Potentiates the Injury Caused by MPP (+) on SH-SY5Y Cells, Which is Attenuated by the Nitric Oxide Synthases Inhibition. Neurochem Res 2014; 39:2452-64; PMID:25297574; http://dx.doi.org/10.1007/s11064-014-1449-1

[42] Tsou Y-H, Shih C-T, Ching C-H, Huang J-Y, Jen CJ, Yu L, Kuo YM, Wu FS, Chuang JI. Treadmill exercise activates Nrf2 antioxidant system to protect the nigrostriatal dopaminergic neurons from MPP+ toxicity. Exp Neurol 2015; 263:50-62; PMID:25286336; http://dx.doi.org/10.1016/j.expneurol.2014.09.021

[43] Chong C-M, Shen M, Zhou Z-Y, Pan P, Hoi P-M, Li S, Liang W, Ai N, Zhang LQ, Li CW, et al. Discovery of a benzofuran derivative (MBPTA) as a novel ROCK inhibitor that protects against MPP+-induced oxidative stress and cell death in SH-SY5Y cells. Free Radical

Bio Med 2014; 74:283-93; PMID:24973649; http://dx.doi.org/10.1016/j.freeradbiomed.2014.06.014

[44] Li W, Yang Q, Mao Z. Chaperone-mediated autophagy: machinery, regulation and biological consequences. Cell Mol Life Sci 2011; 68:749-63; PMID:20976518; http://dx.doi.org/10.1007/s00018-010-0565-6

[45] Liu X, Huang S, Wang X, Tang B, Li W, Mao Z. Chaperone-mediated autophagy and neurodegeneration: connections, mechanisms, and therapeutic implications. Neurosci Bull 2015; 31:407-15; PMID:26206600; http://dx.doi.org/10.1007/s12264-015-1542-8

[46] Cai Z, Zeng W, Tao K, Zhen E, Wang B, Yang Q. Chaperone-mediated autophagy: roles in neuroprotection. Neurosci Bull 2015; 31:452-8; PMID:26206599; http://dx.doi.org/10.1007/s12264-015-1540-x

[47] Gong X, Tang X, Wiedmann M, Wang X, Peng J, Zheng D, Blair LA, Marshall J, Mao Z. Cdk5-mediated inhibition of the protective effects of transcription factor MEF2 in neurotoxicity-induced apoptosis. Neuron 2003; 38:33-46; PMID:12691662; http://dx.doi.org/10.1016/S0896-6273(03)00191-0

[48] Tang X, Wang X, Gong X, Tong M, Park D, Xia Z, Mao Z. Cyclin-dependent kinase 5 mediates neurotoxin-induced degradation of the transcription factor myocyte enhancer factor 2. J Neurosci 2005; 25:4823-34; PMID:15888658; http://dx.doi.org/10.1523/JNEUROSCI.1331-05.2005

[49] She H, Yang Q, Shepherd K, Smith Y, Miller G, Testa C, Mao Z. Direct regulation of complex I by mitochondrial MEF2D is disrupted in a mouse model of Parkinson disease and in human patients. J Clin Invest 2011; 121:930; PMID:21393861; http://dx.doi.org/10.1172/JCI43871

[50] McCoy MK, Martinez TN, Ruhn KA, Szymkowski DE, Smith CG, Botterman BR, Tansey KE, Tansey MG. Blocking soluble tumor necrosis factor signaling with dominant-negative tumor necrosis factor inhibitor attenuates loss of dopaminergic neurons in models of Parkinson's disease. J Neurosci 2006; 26:9365-75; PMID:16971520; http://dx.doi.org/10.1523/JNEUROSCI.1504-06.2006

[51] Sahay S, Ghosh D, Singh PK, Maji SK. Alteration of structure and aggregation of a-synuclein by familial parkinson's disease associated mutations. Curr Protein Pept Sci 2016; PMID:26972727

[52] Bae JR, Lee BD. Function and dysfunction of leucine-rich repeat kinase 2 (LRRK2): Parkinson's disease and beyond. BMB Rep 2015; 48:243-8; PMID:25703537; http://dx.doi.org/10.5483/BMBRep.2015.48.5.032

[53] Kabuta T, Wada K. Insights into links between familial and sporadic Parkinson's disease: physical relationship between UCH-L1 variants and chaperone-mediated autophagy. Autophagy 2008; 4:827-9; PMID:18635949; http://dx.doi.org/10.4161/auto.6560

[54] Kuo S-H, Orenstein S, Koga H, Tang G, Kanter E, Alcalay R, et al. LRRK2 G2019S impairs chaperone-mediated autophagy in neurons (S13. 003). Neurology 2013; 80:S13. 003; http://www.neurology.org/content/80/7_Supplement/IN2-1.001.abstract

[55] Son JH, Chun HS, Joh TH, Cho S, Conti B, Lee JW. Neuroprotection and neuronal differentiation studies using substantia nigra dopaminergic cells derived from transgenic mouse embryos. J Neurosci 1999; 19:10-20; PMID:9870933

[56] Cuervo AM, Stefanis L, Fredenburg R, Lansbury PT, Sulzer D. Impaired degradation of mutant alpha-synuclein by chaperone-mediated autophagy. Science (New York, NY) 2004; 305:1292-5; PMID:15333840; http://dx.doi.org/10.1126/science.1101738

[57] Trudeau K, Molina AJ, Guo W, Roy S. High glucose disrupts mitochondrial morphology in retinal endothelial cells: implications for diabetic retinopathy. Am J Pathol 2010; 177:447-55; PMID:20522647; http://dx.doi.org/10.2353/ajpath.2010.091029